Air Quality, Atmosphere & Health
https://doi.org/10.1007/s11869-021-00977-0

The impact of biogenic emissions on ozone formation in the Yangtze River Delta region based on MEGANv3.1

Yangjun Wang[1] · Xingjian Tan[1] · Ling Huang[1] · Qian Wang[1] · Hongli Li[1] · Hongyan Zhang[2] · Kun Zhang[1] · Ziyi Liu[1] · Dramane Traore[1] · Elly Yaluk[1] · Joshua S. Fu[3] · Li Li[1]

Received: 3 August 2020 / Accepted: 1 January 2021

Abstract

Biogenic volatile organic compounds (BVOCs) play an important role in atmospheric chemistry due to their large quantities and high reactivity. In this study, the impacts of BVOC emissions on ozone formation were investigated based on MEGANv3.1 in the Yangtze River Delta (YRD) region, which has increasingly suffered from ozone pollution in recent years. The sensitivities of BVOC emissions to different drought stress configurations and the quality of emission factors were evaluated. Furthermore, BVOC contribution to ozone formation was simulated by integrated meteorology and air quality model system and the impacts of different BVOC emission scenarios on ozone concentration were discussed. Annual BVOC emissions estimated with the default drought stress configuration (i.e., base case) was 6.8×10^5 tons. The drought stress algorithm implemented in MEGANv3.1 could suppress BVOC emissions by 58% and this algorithm was sensitive to the choice of wilting point values. The BVOC contribution to the average of daily maximum 8 h ozone concentration without drought stress effect in July 2016 was 104% higher than that in the base scenario when the drought stress effect is activated. Using an alternative set of wilting point led to BVOC contribution being 48% higher than that in the base scenario. High contributions of BVOCs to simulated ozone concentration were found in northern Zhejiang, especially in Hangzhou and its surrounding areas.

Keywords BVOCs · MEGAN · Drought response · Ozone

Introduction

Volatile organic compounds (VOCs) are important precursors for the formation of secondary organic aerosols (SOA) and ozone (O_3), which have adverse impacts on public health (Castell et al. 2008), global and regional climate change (Arneth et al. 2007), and visibility (Park et al. 2004). VOCs are emitted from anthropogenic activities (AVOCs) and natural sources. At the global scale, VOC emissions from natural sources (90% are emitted by vegetation) have far exceeded those from anthropogenic sources (Qu et al. 2013; Guenther et al. 1995). Vegetation-emitted VOCs are referred to as biogenic emissions (BVOCs), of which isoprene, monoterpenes, and sesquiterpenes are the dominant species (Isidorov et al. 1985; Sakulyanontvittaya et al. 2008).

BVOC emissions are an essential input to air quality models for the simulation of secondary air pollutants, such as ozone. A series of models, including the Biogenic Emissions Inventory System (BEIS1 and BEIS2, Pierce and Waldruff 1991; Pierce et al. 1998), the Global Emission Inventory

Highlights 1. Implementing drought stress algorithm in MEGANv3.1 could suppress BVOC emissions by 35~58%;
2. The impacts of drought stress on BVOC emissions are closely related with the choice of wilting point;
3. Impacts of BVOC emissions on ozone formation were most significant in Hangzhou and surrounding areas.

✉ Ling Huang
linghuang@shu.edu.cn

✉ Li Li
lily@shu.edu.cn

[1] School of Environmental and Chemical Engineering, Shanghai University, Shanghai 200444, China

[2] School of Computer, Henan University of Engineering, Zhengzhou 451191, China

[3] Department of Civil and Environmental Engineering, University of Tennessee, Knoxville, TN, USA

Published online: 01 March 2021

Activity (G95, Guenther et al. 1995), the Global Biosphere Emissions and Interactions System (GLOBEIS, Guenther et al. 1999a, b), and the Model of Emissions of Gases and Aerosols from Nature (MEGAN, Guenther et al. 2006), have been developed to estimate BVOC emissions. Different models can lead to substantial differences in predicted BVOC emissions, even by more than a factor of 2 (Warneke et al. 2010), resulting in large uncertainties of subsequent air quality simulations (Li et al. 2011; Thunis et al. 2012). Compared to the BEIS models, which were designed for regulatory purposes based on fixed land cover and parameters, MEGAN was intended for a more flexible use for both regulatory and research purposes (Guenther et al. 2006). The most widely used version of the MEGAN model is version 2.1 (Guenther et al. 2012), which has been used in numerous studies worldwide (e.g., Chi and Xie 2012; Wentao and Shanlun 2012; Situ et al. 2013). In China, MEGAN was applied in various studies, especially for densely populated and economically developed regions, such as the Yangtze River Delta (YRD) region (e.g., Liu et al. 2018; Song et al. 2012) and the Pearl River Delta (PRD) region (e.g., Situ et al. 2013; Wang et al. 2011; Zheng et al. 2010).

An updated version of the MEGAN (MEGANv3) was developed in 2017 with the aim to better represent emission responses to environmental stress (Guenther et al. 2017). A more recent version of MEGAN (MEGANv3.1) was released in 2019 and the updates for this version are mainly related to the soil NOx algorithm (Guenther et al. 2019). Thus, we refer to the latest MEGAN version as MEGANv3.1 throughout this study. Compared with MEGANv2.1, there are three major updates in MEGANv3.1 (Guenther et al. 2019). Firstly, the canopy environment model was updated by modification and/or addition of three new procedures to improve the representation of the canopy process, including leaf energy balance (using leaf temperature instead of air temperature), canopy gaps (transparency), and emission capacity varying by canopy depth. Secondly, the MEGAN Emission Factor Preprocessor (MEGAN-EFP) was introduced in MEGANv3.1 to help provide suitable emission factor data. The third major update in MEGANv3.1 is to improve the emission activity response by incorporating the drought response algorithm, which is not available in the offline version of MEGANv2.1. In addition to these updates mentioned above, MEGANv3.1 expands the number of VOC species from 150 in MEGANv2.1 to 201 and adds several new emission categories including light hydrocarbons and oxidation products.

Simulated BVOC emissions are influenced by a range of environmental factors, among which the impact of drought is frequently discussed and associated with large uncertainties (Pegoraro et al. 2004). Extended periods of drought have been shown to reduce emissions of isoprene (Brüggemann and Schnitzler 2002; Funk et al. 2005; Sharkey and Loreto 1993) and monoterpenes (Niinemets 2010), while mild drought could lead to an initial increase of isoprene emissions due to increased leaf temperature, which is caused by reducing water loss through transpiration (Sharkey and Loreto 1993; Pegoraro et al. 2004; Beckett et al. 2012). Grote et al. (2009) developed a modeling approach and estimated the effects of drought on photosynthesis and emissions. Pegoraro et al. (2004) revealed that drought stress was a useful parameter in isoprene emission models to illustrate the effect of leaf water potential on isoprene emission strength. Therefore, the uncertainties of simulated BVOC emissions can be greatly reduced by taking the drought response into account if there are large droughts occurring in the modeling domain.

As one of the most urbanized and populated areas in China, the YRD region has suffered high ground-level ozone concentrations in recent years (Lee et al. 2014; Tao et al. 2003). Ozone pollution days over the YRD region increased by 170% from 2014 to 2017 (Liu et al. 2020). As $PM_{2.5}$ (particulate matter with an aerodynamic diameter less than 2.5 μm) concentrations have been steadily decreasing in the YRD region (Li et al. 2019), ozone is becoming an increasingly important air pollutant. With the emphasis on sustainable development, the vegetation coverage of the YRD region increased slowly from 2009 to 2013, and became stable in recent years (Zhou et al. 2012). Due to the dense vegetation coverage in the YRD region, contribution of BVOC emissions to ozone concentrations could be substantial (Liu et al. 2018). However, substantial efforts are needed to improve the accuracy of BVOC emission estimates and further to better understand the impact of BVOCs on ozone pollution in the YRD region.

In this work, the sensitivities of BVOC emission to different drought stress configurations and the choice of quality of the emission factor were investigated utilizing the latest version of MEGAN for the YRD region. The impacts of BVOC emissions on ozone formation with different emission scenarios were quantified using an integrated meteorology and air quality model system. Our results could provide useful information regarding the future control policy related to ozone mitigation.

Methodology

Modeling system

The modeling systems used in this study include MEGANv3.1, the Weather Research Forecasting (WRF) model, and the Comprehensive Air Quality model with Extensions (CAMx), which were used to simulate the BVOC emissions, meteorological fields, and air quality, respectively. For estimating the annual biogenic emissions over the YRD

region, WRF and MEGAN simulations were conducted for January, April, July, and October in 2016. The sensitivities of BVOC emissions to different model parameters are based on simulations for July 2016 only. Figure 1 shows the modeling domain used in this study: the outermost domain (D01), with a horizontal grid spacing of 36 km, covers most areas of China; the middle domain (D02), with a horizontal grid spacing of 12 km, covers the eastern part of China; the innermost domain (D03) with a horizontal grid spacing of 4 km, includes the YRD region which is composed of Jiangsu, Zhejiang, Anhui, and Shanghai. Input data to drive MEGANv3.1 include meteorology (e.g., temperature, solar radiation, relative humidity, soil moisture), leaf area index (LAI), and three types of land cover data (i.e., ecotype, growth form, and relative vegetation composition for each ecotype/growth form). Meteorological data are obtained from the WRF simulation results. LAI data were obtained from the GLASS LAI product (MOD15A2 2017) provided by Global Land Cover Facility with a spatial resolution of 0.05° and a temporal resolution of 8 days. Default land cover data provided by MEGANv3.1 was utilized. Details regarding the configurations of the integrated WRF/CAMx modeling system could be found in our previous study (Li et al. 2020).

Drought response of BVOC emissions

MEGAN estimates biogenic VOC emission rates as the product of an emission factor and an emission activity factor (Guenther et al. 2012):

$$\text{Emission} = \varepsilon \bullet \gamma \bullet \rho \quad (1)$$

where ε ($mg \cdot m^{-2}\ h^{-1}$) is an emission factor that reflects emission rate at standard conditions; ρ represents the production and consumption within the canopy and is usually set as 1. The emission activity factor (γ) accounts for emission responses to changes in environmental and phenological conditions and it is calculated as:

$$\gamma_i = C_{CE} \bullet LAI \bullet \gamma_{P,i}\gamma_{T,i}\gamma_{A,i}\gamma_{SM,i}\gamma_{C,i} \quad (2)$$

where the activity factor for each compound class (i) represents emission response to light (γ_P), temperature (γ_T), leaf age (γ_A), soil moisture (γ_{SM}), LAI, and CO_2 inhibition (γ_C). The canopy environment coefficient (C_{CE}) is assigned a value that results in $\gamma = 1$ for the standard conditions and is dependent on the canopy environment model being used (Guenther et al. 2012). In many applications of MEGANv2.1, the soil moisture and CO_2 inhibition activity factor were ignored (Guenther et al. 2012; Sindelarova et al. 2014).

The drought response of BVOC emissions was simulated by Eq. (3), which involves the soil moisture (θ, $m^3 \cdot m^{-3}$) and the wilting point (θ_w, $m^3 \cdot m^{-3}$, the threshold of soil moisture where plants are unable to further extract any water from the soil). $\Delta\theta_1$ is an empirical parameter which is equal to 0.04 $m^3 \cdot m^{-3}$ and θ_1 is equal to $\theta_w + \Delta\theta_1$.

$$\begin{cases} \gamma_{SM} = 1\ (\theta > \theta_1) \\ \gamma_{SM} = (\theta - \theta_w)/\Delta\theta_1\ (\theta_w < \theta < \theta_1) \\ \gamma_{SM} = 0\ (\theta < \theta_w) \end{cases} \quad (3)$$

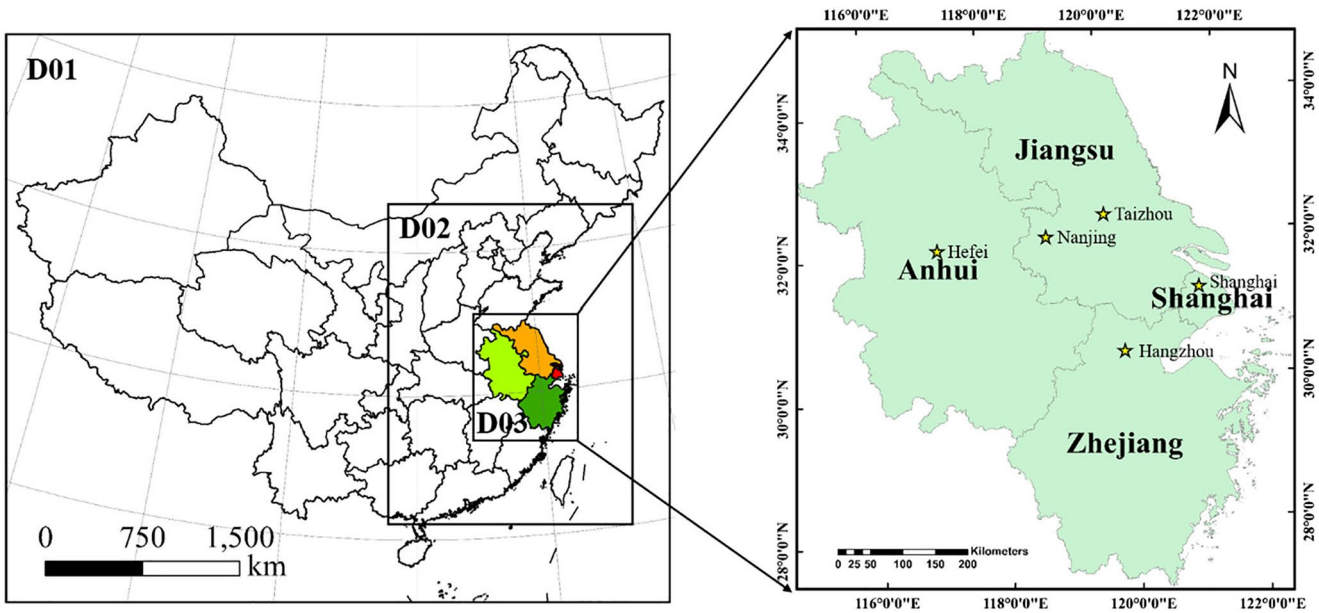

Fig. 1 Simulation domains in this study

In this study, two sets of wilting point data were used: the default values provided by MEGANv3.1 (θ_{w1}) and the other obtained from the study of Chen and Dudhia (2001) (θ_{w2}) (Table 1). The default wilting point values are on average 2.5 times higher than θ_{w2}, indicating that more soil moisture is needed to sustain plant growth under the default setting.

Scenario setup

Four scenarios were designed to analyze the impact of model parameters on simulated BVOC emissions (Table 2). In MEGANv3.1, five levels of emission factor quality (J) are available with J = 4 corresponding to the highest quality and J = 0 to the lowest quality. In this study, only the highest (J = 4) and lowest quality (J = 0) were used. Sce.1 was regarded as the base case scenario where we used the highest quality for emission factor (J = 4) and turned on the drought stress algorithm with the default wilting point values provided by MEGANv3.1. The other three scenarios were conducted to evaluate the simulated emission response to different choices of emission factor quality (Sce.1 vs. Sce.2) and to drought parameterizations (Sce.1 vs. Sce.3 vs. Sce.4). Note that these four scenarios were conducted for July only given that BVOC emissions are highest during summer.

In order to evaluate the impact of BVOCs on ozone formation, four simulations were conducted for July 2016 based on WRF/CAMx with all configurations identical except for the BVOC emissions. For the first three simulations, the estimated BVOC emissions from Sce.1, Sce.4, and Sce.3 in Table 2 were used, corresponding to S_{SM1}, S_{SM2}, and $S_{nostress}$, respectively. A fourth simulation ($S_{noMEGAN}$) was conducted where BVOC emissions were excluded. By comparing the results of these simulations, the impacts of BVOC emissions on the ozone concentration under different emission scenarios could be quantified over the YRD region.

Table 1 Two sets of values for wilting point used in MEGANv3.1 simulation in this study

Soil type	θ_{w1} ($m^3 \cdot m^{-3}$)	θ_{w2} ($m^3 \cdot m^{-3}$)	Relative differences (%)
Sand	0.068	0.010	85.3
Loamy sand	0.075	0.028	62.7
Silt loam	0.144	0.047	67.4
Silt	0.179	0.084	53.1
Loam	0.155	0.084	45.8
Sandy clay loam	0.175	0.066	62.3
Silty clay loam	0.218	0.067	69.3
Clay loam	0.250	0.120	52.0
Sandy clay	0.219	0.103	53.0
Silty clay	0.283	0.100	64.7
Clay	0.286	0.126	55.9
Organic material	0.286	0.138	51.8
Water	0.286	0.060	79.0
Bedrock	0.286	0.094	67.1
Other (land-ice)	0.286	0.028	90.2

Table 2 Configurations of model parameters for scenarios

Scenario no.	Quality options of emission factor	Drought stress	Wilting point
Sce.1 (base case)	J = 4	Yes	Default (θ_{w1})
Sce.2	J = 0	Yes	Default (θ_{w1})
Sce.3	J = 4	No	-
Sce.4	J = 4	Yes	Chen and Dudhia (2001) (θ_{w2})

Results and discussion

Biogenic emissions estimated by MEGANv3.1

The spatial distributions of total BVOC, isoprene, and terpene emissions estimated in the base case scenario (Sce.1) over the YRD region are shown in Fig. 2. Similar to the results of Liu et al. (2018), BVOC emissions are mainly distributed in the southern part of Anhui province and the northern part of Zhejiang province. This spatial pattern follows the distribution of trees (Fig. S1) since trees have relatively higher emission factors than other vegetation. BVOC emissions showed strong seasonal variations with the highest emissions in summer (July, 78.9%) due to high temperature/solar radiation and abundant leaf mass, and lowest in winter (January, 0.9%). In addition, it also exhibited significant diurnal variations (Fig. S2), of which emission rate peaked at 11:00 local time and negligible emissions during night.

The estimated emissions and composition of BVOC species for July 2016 over the YRD region are shown in Fig. S3 and Fig. S4. Annual total emissions (calculated as sum of 4 months multiplied by 3 in Sce.1) of isoprene (ISOP), monoterpenes (TERP), sesquiterpene (SQT), and other BVOCs were estimated to be 2.8×10^5 (41.6% of total BVOCs), 1.1×10^5 (16.7%), 0.24×10^5

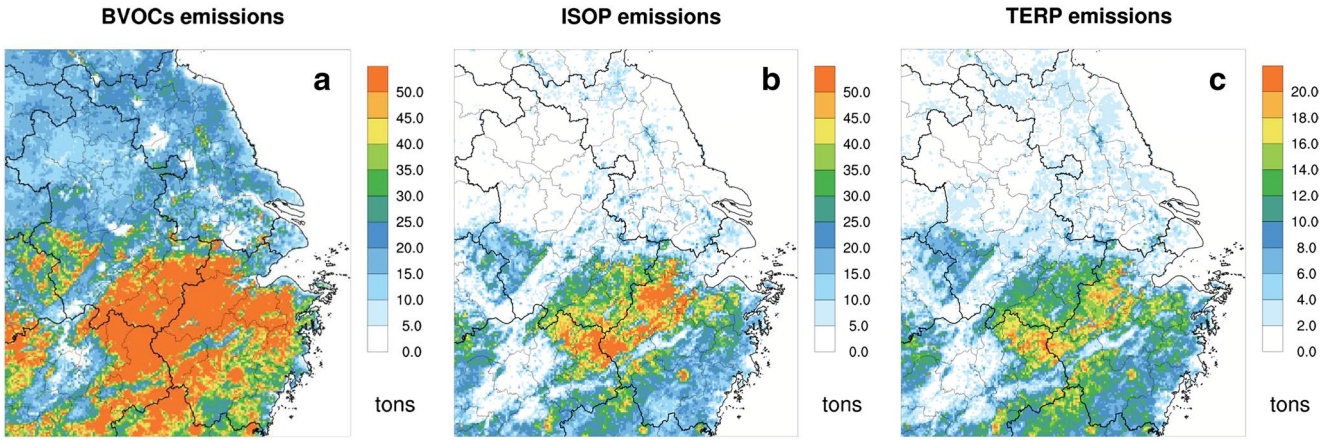

Fig. 2 Spatial distribution of total (**a**) BVOC, (**b**) isoprene, and (**c**) terpene emissions over the YRD region of Sce.1 in 2016

(3.5%), and 2.6×10^5 (38.2%) tons, respectively. Among other BVOCs, methanol is the most abundant species (accounting for 27.7% of other BVOCs), followed by acetone, propene, ethane, ethane, acetaldehyde, and ethanol, together accounting for 48.2% of other BVOCs. Spatial distributions of ISOP and TERP emissions are mainly distributed in the southern part of Anhui and the northern part of Zhejiang, while SQT and OTHER emissions are relatively uniform across YRD (Fig. S5). The main sources of BVOC emissions in Zhejiang and Anhui provinces are trees, which are major emitters to both isoprene and monoterpenes. Shrubs are the main source of BVOC emissions in Shanghai (accounting for 56%), followed by crops (21%) and herbs (17%). BVOC emissions in Jiangsu are mainly from crops and shrubs, each contributing 47% and 29%, respectively.

The annual total BVOC emissions simulated in the base case scenario was 6.8×10^5 tons for year 2016. Compared with existing studies (Table 3), the emission rate of BVOCs in YRD in this study is 1.9 t/(km^2 a), which is much lower than the simulated results reported by Song et al. (2012, lower by 38%) and Liu et al. (2018, lower by 64%). The substantial differences seen between this study and previous studies are partly due to different years being modeled. However, the major cause for these differences is related to the drought stress algorithm implemented in MEGANv3.1, which will be discussed in the following.

Sensitivities of biogenic emissions to different model configurations

J0 vs. J4

Emission factor (EF) is a critical parameter in estimating BVOC emissions and is associated with large uncertainties. The newly added emission factor processor (MEGAN-EFP) enables the user to add/omit emission factors based on experience. In order to look at the uncertainties associated with different quality of the EF data, a second simulation was conducted (Sce.2) by only changing the J values (J = 0) while keeping other settings unchanged. In this case, only isoprene and monoterpene emissions are affected. Figure 3 shows

Table 3 Comparison of simulated BVOC emissions in YRD and PRD

Region	BVOC emissions ($\times 10^4$ t)	Simulated year	Area (km^2)	BVOC emission rate (t/km^2·a)	Reference
YRD	68	2016	3.6×10^5	1.9	Sce.1 in this study (default drought stress)
YRD	162	2016	3.6×10^5	4.5	Sce.3 in this study (without stress)
YRD	188.6	2014	3.6×10^5	5.2	Liu et al. (2018)
YRD	110	2010	3.6×10^5	3.1	Song et al. (2012)
PRD	19.6	1998	5.8×10^4	3.4	Yang et al. (2001)
PRD	33.9	2006	5.3×10^4	6.4	Wang et al. (2011)
PRD	30	2006	4.7×10^4	6.3	Zheng et al. (2010)

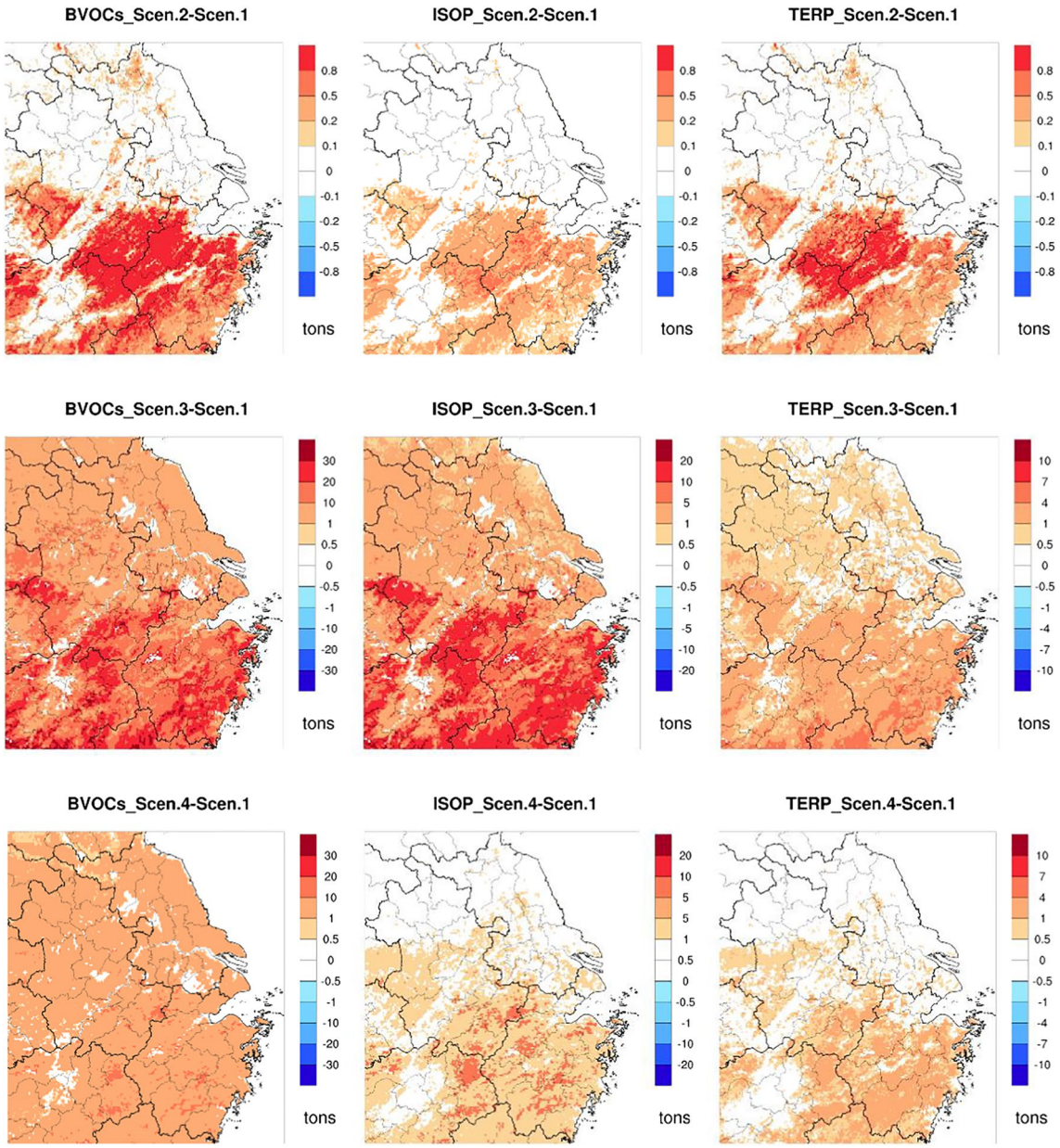

Fig. 3 Spatial distribution of emission differences of total BVOCs, isoprene, and monoterpenes between different scenarios over the YRD region in July 2016

the spatial differences of isoprene and monoterpene emissions between the two scenarios. Using lower quality EF data (J = 0) tends to result in slightly higher EF values, and therefore slightly higher BVOC emissions by 4.4%. BVOC emissions of Zhejiang province in Sce.2 increased by 6% while emissions in Shanghai increased by less than 0.5%. Spatial distributions of isoprene and monoterpene emissions stay the same as changing J values only changes the magnitudes of emissions.

Drought responses of BVOC emissions

In order to investigate model sensitivities to different drought parameterizations, two more scenarios were conducted: Sce.3 where the drought-induced stress option was turned off and Sce.4 where a different set of wilting point data for drought impact parameterization was used.

Spatial distributions of BVOC emissions estimated in Sce.3 and Sce.4 are consistent with the spatial distribution of Sce.1, where high isoprene emissions are displayed over

Zhejiang province and the southern part of Anhui province and monoterpene emissions with same distribution characteristics. However, in terms of emission magnitudes, using different drought parameterizations could lead to significant differences in estimated biogenic emissions (Fig. 3). When the drought stress was ignored (Sce.3), total BVOC emissions were increased by 137% compared to the base case scenario, where the MEGANv3.1 default wilting point was used. The substantial increase in BVOC emissions is mainly associated with increase in isoprene and monoterpene emissions, which increased by 147% and 117%, respectively. Shanghai shows the biggest increase of BVOC emissions by 173%, followed by Anhui province (152%). If drought stress is not considered, the annual BVOCs is estimated to be 4.5 t/(km^2 a), which is comparable to numbers reported by previous results (Table 3). The parameterization of drought stress is very sensitive to the choice of the wilting point values. Estimated total BVOC emissions when using an alternative set of wilting point values (Sce.4) were 54% higher than those of Sce.1. Isoprene and monoterpene emissions were 54% and 50% higher in Sce.4, respectively.

Our modeling results indicate that the soil algorithm implemented in MEGANv3.1 could lead to substantial suppression of BVOC emissions and this algorithm is extremely sensitive to the choice of the wilting point values. Potosnak et al. (2014) used the witling point values (0.08) from Chen and Dudhia (2001) at the MOFLUX site and reported no effect of drought stress on the simulated isoprene emissions in 2011 and 2012 simply because this wilting point is too low. Seco et al. (2015) used a wilting point value of 0.23, which is a more representative value for the soil type at the same site, and found that the wilting point value can explain most of the effects of drought on isoprene emissions. Müller et al. (2007) found that when using the ECMWF (European Centre for Medium-Range Weather Forecasts) global weather model, it was necessary to use the ECMWF wilting point dataset. Previous studies (Liu et al. 2018; Song et al. 2012; Wang et al. 2011; Zheng et al. 2010) based on MEGANv2.1 simply ignore the drought stress, and the accuracy and representativeness of the wilting point data have not been much studied, especially in China. Jiang et al. (2018) developed a mechanistic representation of drought impacts on isoprene emissions with the focus of algorithm development that considers both photosynthesis and water stress simultaneously, and the accuracy of the wilting point was not addressed. Therefore, in order to better represent drought stress on predicted BVOC emissions, further studies on local wilting point values are needed.

Impacts of BVOC emissions on ozone

We further conducted a series of air quality simulations with different BVOC emissions for July 2016 to investigate the impact of BVOC emissions on ozone formation. Evaluation of the model performances is discussed in the supplemental information. Basically, values of the index of agreement (IOA) at the five selected stations ranged from 0.8 to 0.9. The model tends to overpredict ozone concentrations with a normalized mean bias (NMB) by − 3.0~34.0%.

Monthly average spatial distributions of simulated ozone concentration in the base scenario (S_{SM1}) are shown in Fig. 4 for (a) daily maximum hourly concentration and (b) daily average of maximum 8 hourly concentrations, respectively. In this case, BVOC emissions are estimated with the default MEGAN wilting point values. Spatially, simulated ozone concentrations exhibit a decreasing trend from north to south, which is different from the spatial distribution of BVOC emissions. Relatively high ozone concentrations mainly concentrated in the coastal areas of Jiangsu province and bordering regions of southern Jiangsu, northern Zhejiang, and western Shanghai. Sparse locations of high ozone concentration were also observed, likely due to large precursor emissions from point sources.

Figure 5 showed the BVOC contribution (S_{SM1}−$S_{noMEGAN}$) to ozone formation in the YRD region for July 2016. The biggest simulated ozone contribution from BVOCs was noticed in northern Zhejiang, especially in Hangzhou and its surrounding areas, with maximum ozone contribution over 26 μg/m^3 for the max 8-h average concentration. Domain-averaged ozone contribution from BVOC emissions was estimated to be 5.6 μg/m^3 and 5.0 μg/m^3 for daily maximum hourly concentration and max 8-h average concentration, respectively. As illustrated in Fig. 6, different drought configurations associated with the estimation of BVOC emissions could have substantial impacts on simulated ozone concentrations. When using the alternative set of wilting point values instead of the default values, domain-wide BVOC emissions increased by 53.9% and the contribution to the daily maximum 8-h ozone concentration increased by 52.5%, with maximum absolute increase in ozone contribution exceeding 13.2 μg/m^3. If no drought stress is included, BVOC contribution to ozone concentration would increase by 116.2% on average.

We further looked at the simulated ozone concentrations for five cities: Shanghai, Nanjing, Taizhou, Hangzhou, and Hefei (see locations in Fig. 1). In the base case simulation (S_{SM1}), the contributions of BVOC emissions to monthly averaged ozone concentration range 6.4~16.3% (Fig. 7). When an alternative set of wilting

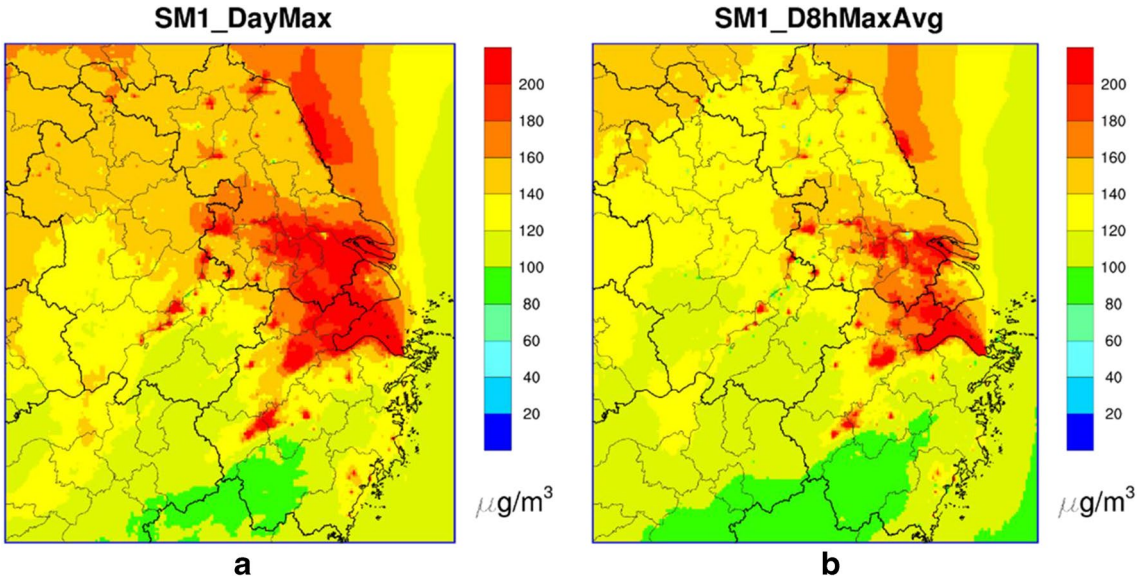

Fig. 4 Average spatial distribution of ozone concentration in base scenario for (**a**) daily max hourly concentration and (**b**) daily average of max 8 hourly concentrations in July 2016

point values is used, BVOC contributions to monthly averaged ozone range 9.6~21.0%. If no drought stress is considered ($S_{nostress}$), BVOC contribution to ozone formation is highest, ranging 13.3~25.8%. Among the five cities, BVOC emissions in Hangzhou exhibit the highest contributions.

The impact of BVOCs during an ozone episode

Based on the simulation results of the base scenario, high concentrations of ozone were found in the YRD region during the period from July 25 to July 30, 2016. During this period, observed daily maximum 8-h ozone concentration ranges from 69.3 μg/m^3 in Anqing on July 27 to 259.8 μg/m^3 in Taizhou (Jiangzu province) on July 25. Spatial distribution of observed daily maximum 8-h ozone concentrations are illustrated in Fig. S6. On July

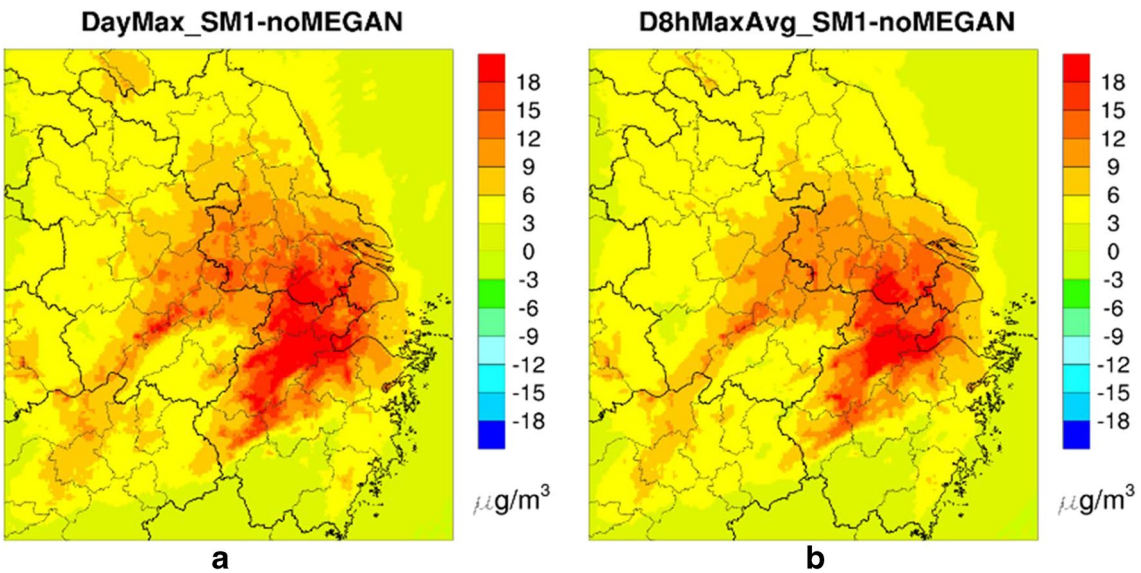

Fig. 5 Average spatial distribution of ozone concentration contributed from BVOC emissions for (**a**) maximum hourly concentration and (**b**) avg maximum 8 hourly concentrations in July 2016, respectively

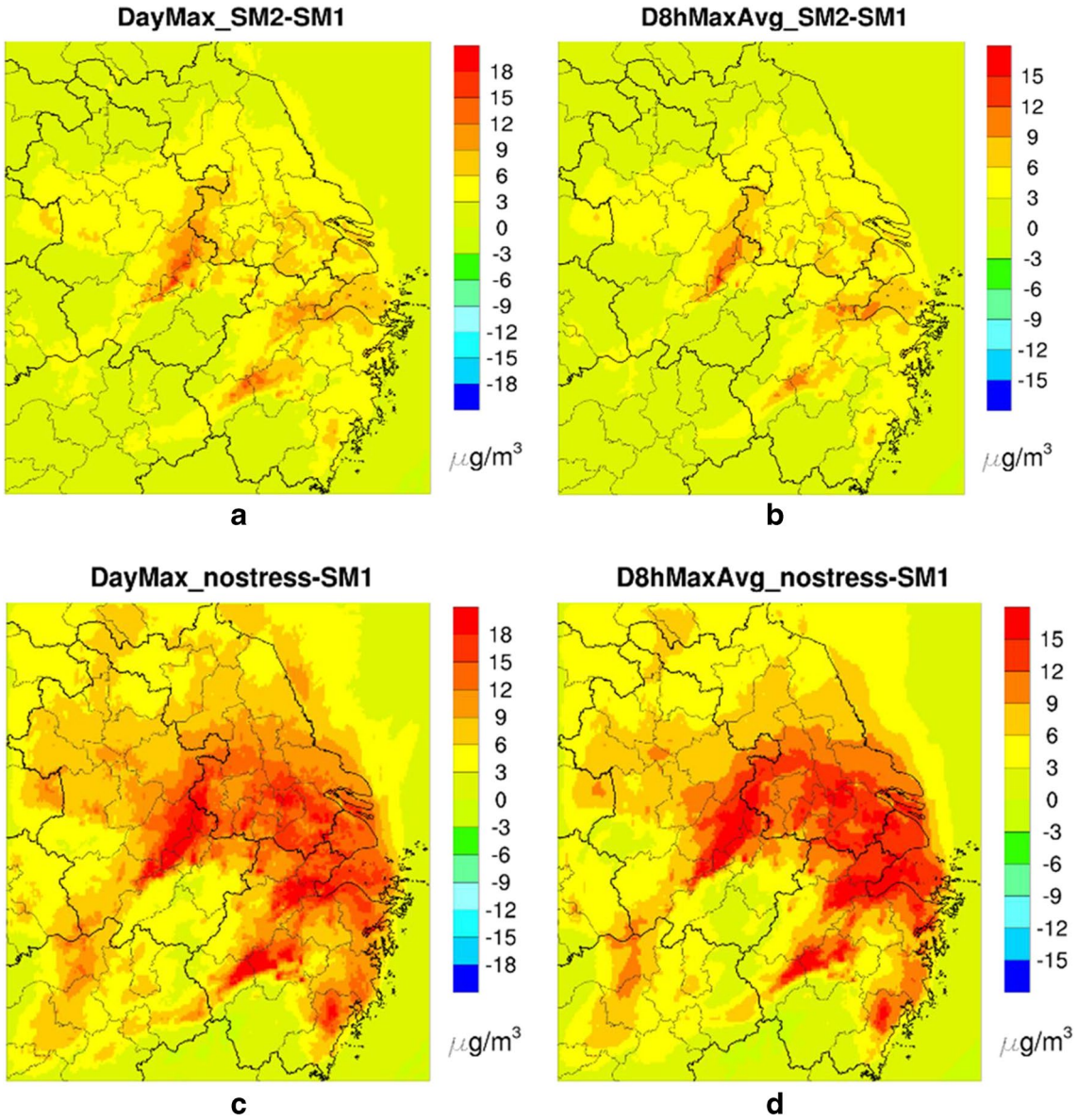

Fig. 6 Spatial distribution averaged ozone differences for July 2016. Top panels show the difference between S_{SM1} and S_{SM2} for (**a**) maximum hourly concentration and (**b**) maximum 8 hourly average concentration; bottom panels show the difference between S_{SM1} and $S_{nostress}$ for (**c**) maximum hourly concentration and (**d**) maximum 8 hourly average concentration

29, 19 out of 41 cities in the YRD region exceed the national standard for ambient ozone (i.e., 160 μg/m^3) and these cities are mainly located in southern Jiangsu and northern Zhejiang province. Figure S7 showed the daily average of simulated maximum 8-h ozone concentration during this time period. Similar to the monthly averages, the high ozone mainly concentrated in the central and coastal areas of the YRD region, including northern Zhejiang, southern Jiangsu, Shanghai, and a small part of eastern Anhui. Domain-averaged 8-h ozone concentration exceeded 165 μg/m^3. During this time period, the YRD region experienced continuous high temperatures with daily averaged temperature exceeding 30 ℃, resulting in the increase of BVOC emissions as well as faster photochemical reactions.

Among the five selected cities, the contribution of ozone from BVOCs in Taizhou, which is a city in northern Jiangsu, was relatively low (< 10%; Fig. 8). On the 25th and 30th, ozone concentrations resulting from BVOC emissions in Shanghai were particularly low, which could be related to the transport of the ocean air mass. The contribution of ozone from BVOCs exceeded 10% in Nanjing for 2 days. The contributions of BVOCs to ozone concentration in Hangzhou were always high

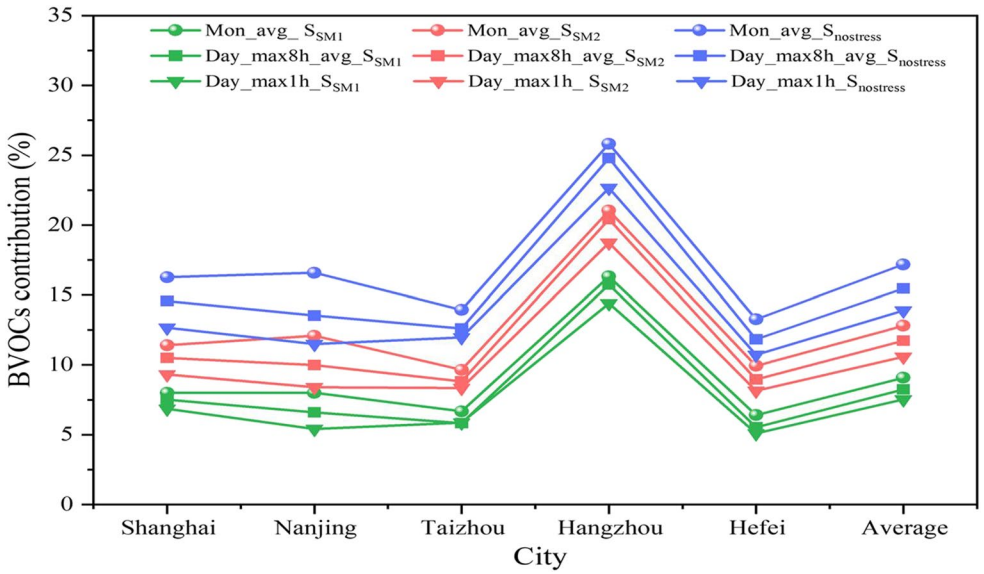

Fig. 7 Variation of BVOC contribution percentages to the average ozone concentration in some cities in the YRD region in July 2016

(8.9~34.7%). On July 27, the contribution of BVOC emissions in Hangzhou reached a maximum of 34.7%. The high contribution of BVOCs to ozone concentration simulated in Hangzhou during the selected period is mainly caused by the fact that BVOC emissions in Hangzhou are the highest among these cities. For instance, in July, the total BVOC emissions in Hangzhou is estimated to be 10,894 tons, which is 43.3%, 113.3%, 59.3%, and 100.9% higher than those of Shanghai, Hefei, Nanjing, and Taizhou, respectively.

Conclusions

In this study, the latest version of MEGAN was applied to estimate BVOC emissions during 2016 over the YRD region. The sensitivities of BVOC emissions to different drought stress configurations and quality of the emission factor were discussed. With the default drought stress configuration and highest quality of emission factor, the annual BVOC emissions over the YRD region was estimated to be 6.8×10^5 tons. Changing the quality level of emission factor led to negligible differences in estimated biogenic emissions (relative differences < 5%). On the contrary, the drought stress

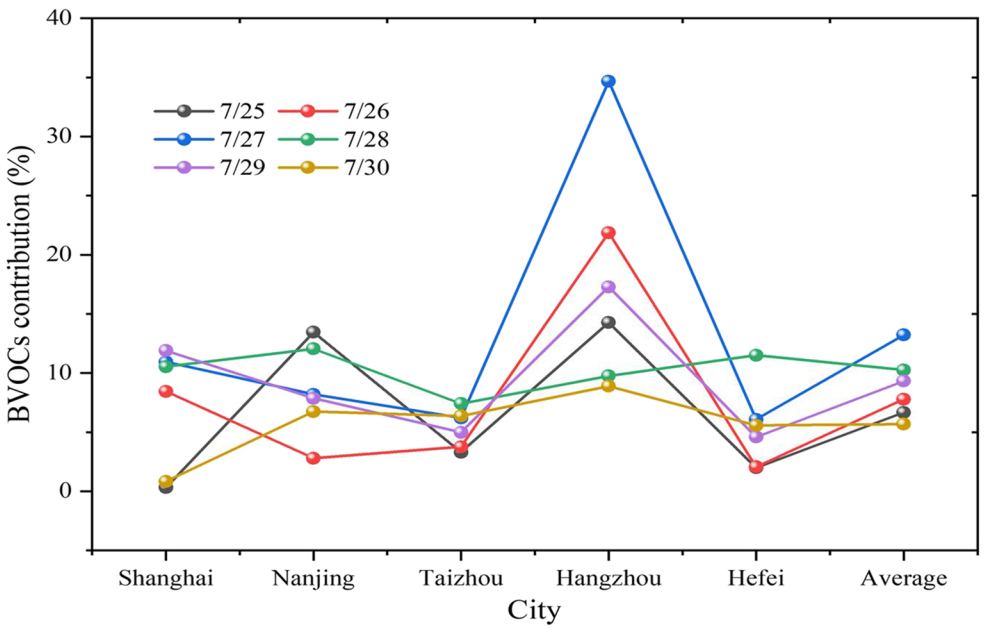

Fig. 8 The contribution percentages of BVOCs to ozone concentrations in cities during the ozone episode from July 25 to July 30, 2016

algorithm exhibited great impacts on simulated BVOC emissions. Turning off the drought stress algorithm led to 137% higher biogenic emissions compared to the default drought stress parameterization. Using an alternative set of wiling point values (on average 64% smaller than default values) leads to 57% higher biogenic emissions. These results indicate that the drought stress algorithm could lead to substantial suppression of BVOC emissions and this algorithm was sensitive to the choice of the wilting point values.

BVOC contribution to ozone formation in the YRD region and the impact from different BVOC emission scenarios were further quantified for July 2016. BVOC contribution to ozone concentration without drought stress effect was 104% higher than that in the base scenario averaged at five selected cities. When BVOC emissions estimated with an alternative set of wilting points were used, ozone contributions from biogenic emissions were 47.9% higher than the base case. Based on the simulation results, the highest ozone contributions from biogenic emissions were found in northern Zhejiang, especially in Hangzhou and its surrounding areas.

Supplementary information The online version contains supplementary material available at https://doi.org/10.1007/s11869-021-00977-0.

Funding This work was supported by the Shanghai Science and Technology Innovation Plan (No. 19DZ1205007), the National Key R&D Program of China (No.2018YFC0213600), Shanghai Sail Program (No. 19YF1415600), and the National Natural Science Foundation of China (No. 41875161, 42005112, 42075144).

Declarations

Conflict of interest The authors have no competing interests.

References

Arneth A, Miller PA, Scholze M et al (2007) CO_2 inhibition of global terrestrial isoprene emissions: potential implications for atmospheric chemistry. Geophys Res Lett 34:L18813. https://doi.org/10.1029/2007GL030615

Beckett M, Loreto F, Velikova V et al (2012) Photosynthetic limitations and volatile and non-volatile isoprenoids in the poikilochlorophyllous resurrection plant Xerophyta humilis during dehydration and rehydration. Plant Cell Environ 35(12):2061–2074

Brüggemann N, Schnitzler JP (2002) Comparison of isoprene emission, intercellular isoprene concentration and photosynthetic performance in water-limited oak (Quercus pubescens Willd. and Quercus robur L.) saplings. Plant Biol 4(4):456–463

Castell N, Stein AF, Salvador R et al (2008) The impact of biogenic VOC emissions on photochemical ozone formation during a high ozone pollution episode in the Iberian Peninsula in the 2003 summer season. Advances in Science and Research 2(1):9–15

Chen F, Dudhia J (2001) Coupling an advanced land surface–hydrology model with the Penn State–NCAR MM5 modeling system. Part I: model implementation and sensitivity monthly. Weather Review 129(4):569–585

Chi YQ, Xie SD (2012) Spatiotemporal inventory of biogenic volatile organic compound emissions in China based on vegetation volume and production. Advanced Materials Research 356–360:2579–2582

Funk JL, Jones CG, Gray DW et al (2005) Variation in isoprene emission from Quercus rubra: sources, causes, and consequences for estimating fluxes. J Geophys Res Atmos. 110(D4)

Grote R, Lavoir AV, Rambal S et al (2009) Modelling the drought impact on monoterpene fluxes from an evergreen Mediterranean forest canopy. Oecologia 160(2):213–223

Guenther A, Nicholas HC, Erickson D et al (1995) A global model of natural volatile organic compound emissions. J Geophys Res Atmos 100(D5):8873–8892

Guenther A, Archer S, Greenberg J et al (1999) Biogenic hydrocarbon emissions and landcover/climate change in a subtropical savanna. Phys Chem Earth (B) 24(6):659–667

Guenther A, Bangh B, Beasseur G et al (1999) Isoprene emission estimates and uncertainties for the central African EXPRESSO study domain. J Geophys Res Atmos 104(D23):30625–30639

Guenther A, Karl T, Harley P et al (2006) Estimates of global terrestrial isoprene emissions using MEGAN (Model of Emissions of Gases and Aerosols from Nature). Atmos Chem Phys 6:3181–3210

Guenther A, Jiang XY, Heald CL et al (2012) The Model of Emissions of Gases and Aerosols from Nature version 2.1 (MEGAN2.1): an extended and updated framework for modeling biogenic emissions. Geosci Model Dev 6:1471–1492

Guenther AB, Shah T, Huang L et al (2017) A next generation modeling system for estimating Texas biogenic VOC emissions [M]. AQRP Project 16-011. Texas Air Quality Research Program (AQRP), The University of Texas at Austin, Austin

Guenther A, Jiang X, Shah T et al (2019) Model of emissions of gases and aerosol from nature version 3 (MEGAN3). In: Air pollution modeling and its application XXVI. Springer,Cham, pp 187

Isidorov VA, Zenkevich IG, Ioffe BV (1985) Volatile organic compounds in the atmosphere of forests. Atmos Environ 19:1–8

Jiang XY, Guenther A, Mark P et al (2018) Isoprene emission response to drought and the impact on global atmospheric chemistry. Atmos Environ 183:69–83

Lee KY, Kwak KH, Ryu YH (2014) Impacts of biogenic isoprene emission on ozone air quality in the Seoul metropolitan area. Atmos Environ 96:209–219

Li L, Chen CH, Huang C et al (2011) Ozone sensitivity analysis with the MM5-CMAQ modeling system for Shanghai. J Environ Sci 23(007):1150–1157

Li J, Liao H, Hu J et al (2019) Severe particulate pollution days in China during 2013–2018 and the associated typical weather patterns in Beijing-Tianjin-Hebei and the Yangtze River Delta regions. Environ Pollut 248(MAY):74–81

Li L, Li Q, Huang L et al (2020) Air quality changes during the COVID-19 lockdown over the Yangtze River Delta Region: an insight into the impact of human activity pattern changes on air pollution variation. Sci Total Environ 732:139282

Liu Y, Li L, An JY et al (2018) Estimation of biogenic VOC emissions and its impact on ozone formation over the Yangtze River Delta region. China Atmos Environ 186:113–128

Liu YX, Zhao QB, Hao X et al (2020) Increasing surface ozone and enhanced secondary organic carbon formation at a city junction site: an epitome of the Yangtze River Delta, China (2014–2017). Environ Pollut 265(Pt A):114847

Müller JF, Stavrakou T, Wallens S et al (2007) Supplement to "Global isoprene emissions calculated based on MEGAN, ECMWF analyses and a detailed canopy environment model". Atmospheric Chemistry & Physics Discussions 7(6)

Niinemets U (2010) Mild versus severe stress and BVOCs: thresholds, priming and consequences. Trends Plant Sci 15(3):145–153

Park RJ, Jacob DJ, Fairlie DT (2004) Natural and transboundary pollution influences on aerosol concentrations and visibility degradation in the United States. J Geophys Res Atmos 134:963–967

Pegoraro E, Rey A, Greenberg J (2004) Effect of drought on isoprene emission rates from leaves of Quercus virginiana Mill. Atmos Environ 38:6149–6156

Pierce T, Waldruff P (1991) PC-BEIS: a personal computer version of the biogenic emissions inventory. System Air Repair 41:937–941

Pierce T, Geron C, Bender L (1998) Influence of increased isoprene emissions on regional ozone modeling. J Geophys Res Atmos 103:25611–25629

Potosnak MJ, LeStourgeon L, Pallardy SG et al (2014) Observed and modeled ecosystem isoprene fluxes from an oak-dominated temperate forest and the influence of drought stress. Atmos Environ 84:314–322

Qu Y, An J, Li J (2013) Synergistic impacts of anthropogenic and biogenic emissions on summer surface O3 in East Asia. J Environ Sci 25:520–530

Sakulyanontvittaya T, Duhl T, Wiedinmyer C et al (2008) Monoterpene and sesquiterpene emission estimates for the United States. Environ Sci Technol 42:1623–1629

Seco R, Karl T, Guenther A et al (2015) Ecosystem-scale volatile organic compound fluxes during an extreme drought in a broadleaf temperate forest of the Missouri Ozarks (central USA). Glob Chang Biol 21(10):3657–3674

Sharkey TD, Loreto F (1993) Water stress, temperature, and light effects on the capacity for isoprene emission and photosynthesis of kudzu leaves. Oecologia 95(3):328–333

Sindelarova K, Granier C, Bouarar I et al (2014) Global data set of biogenic VOC emissions calculated by the MEGAN model over the last 30 years. Atmospheric Chem Phys 14(17):9317–9341

Situ S, Guenther A, Wang X et al (2013) Impacts of seasonal and regional variability in biogenic VOC emissions on surface ozone in the Pearl River delta region China. Atmospheric Chem Phys 13:11803–11817

Song Y, Zhang Y, Wang Q et al (2012) Estimation of biogenic VOCs emissions in Eastern China based on remote sensing data. Acta Sci Circum 32:2216–2227

Tao ZN, Larson SM, Wuebbles DJ et al (2003) A summer simulation of biogenic contributions to ground-level ozone over the continental United States. J Geophys Res 108(D14):4404

Thunis P, Pederzoli A, Pernigotti D (2012) Performance criteria to evaluate air quality modeling applications. Atmos Environ 59:476–482

Wang X, Situ S, Guenther A et al (2011) Spatiotemporal variability of biogenic terpenoid emissions in Pearl River Delta, China, with high-resolution land-cover and meteorological data. Tellus 63(2):241–254

Warneke C, Gouw JAD, Negro LD et al (2010) Biogenic emission measurement and inventories determination of biogenic emissions in the eastern United States and Texas and comparison with biogenic emission inventories. J Geophys Res Atmos 115(D7):D00F18

Wentao N, Shanlun Z (2012) Estimation of Biogenic Isoprene Emission in East Asia. J Green Sci Technol 2012(4):209–212

Zheng J, Zheng Z, Yu Y et al (2010) Temporal, spatial characteristics and uncertainty of biogenic VOC emissions in the Pearl River Delta region. China Atmos Environ 44(16):1960–1969

Zhou F, Xu YP, Lv HH et al (2012) Analysis of the vegetation change in the Yangtze River Delta based on modis-evi time series data. Resour Environ Yangtze Basin 21(11):1363–1369

Terms and Conditions

Springer Nature journal content, brought to you courtesy of Springer Nature Customer Service Center GmbH (“Springer Nature”).
Springer Nature supports a reasonable amount of sharing of research papers by authors, subscribers and authorised users (“Users”), for small-scale personal, non-commercial use provided that all copyright, trade and service marks and other proprietary notices are maintained. By accessing, sharing, receiving or otherwise using the Springer Nature journal content you agree to these terms of use (“Terms”). For these purposes, Springer Nature considers academic use (by researchers and students) to be non-commercial.
These Terms are supplementary and will apply in addition to any applicable website terms and conditions, a relevant site licence or a personal subscription. These Terms will prevail over any conflict or ambiguity with regards to the relevant terms, a site licence or a personal subscription (to the extent of the conflict or ambiguity only). For Creative Commons-licensed articles, the terms of the Creative Commons license used will apply.
We collect and use personal data to provide access to the Springer Nature journal content. We may also use these personal data internally within ResearchGate and Springer Nature and as agreed share it, in an anonymised way, for purposes of tracking, analysis and reporting. We will not otherwise disclose your personal data outside the ResearchGate or the Springer Nature group of companies unless we have your permission as detailed in the Privacy Policy.
While Users may use the Springer Nature journal content for small scale, personal non-commercial use, it is important to note that Users may not:

1. use such content for the purpose of providing other users with access on a regular or large scale basis or as a means to circumvent access control;
2. use such content where to do so would be considered a criminal or statutory offence in any jurisdiction, or gives rise to civil liability, or is otherwise unlawful;
3. falsely or misleadingly imply or suggest endorsement, approval , sponsorship, or association unless explicitly agreed to by Springer Nature in writing;
4. use bots or other automated methods to access the content or redirect messages
5. override any security feature or exclusionary protocol; or
6. share the content in order to create substitute for Springer Nature products or services or a systematic database of Springer Nature journal content.

In line with the restriction against commercial use, Springer Nature does not permit the creation of a product or service that creates revenue, royalties, rent or income from our content or its inclusion as part of a paid for service or for other commercial gain. Springer Nature journal content cannot be used for inter-library loans and librarians may not upload Springer Nature journal content on a large scale into their, or any other, institutional repository.
These terms of use are reviewed regularly and may be amended at any time. Springer Nature is not obligated to publish any information or content on this website and may remove it or features or functionality at our sole discretion, at any time with or without notice. Springer Nature may revoke this licence to you at any time and remove access to any copies of the Springer Nature journal content which have been saved.
To the fullest extent permitted by law, Springer Nature makes no warranties, representations or guarantees to Users, either express or implied with respect to the Springer nature journal content and all parties disclaim and waive any implied warranties or warranties imposed by law, including merchantability or fitness for any particular purpose.
Please note that these rights do not automatically extend to content, data or other material published by Springer Nature that may be licensed from third parties.
If you would like to use or distribute our Springer Nature journal content to a wider audience or on a regular basis or in any other manner not expressly permitted by these Terms, please contact Springer Nature at

onlineservice@springernature.com